

A Molecular Dynamics Study of Aqueous Solutions.

VIII. Improved Simulation and Structural Properties of a NH_4Cl Solution

Gy. I. Szász and K. Heinzinger

Max-Planck-Institut für Chemie, (Otto-Hahn-Institut), Mainz, Germany

Z. Naturforsch. **34a**, 840–849 (1979); received April 26, 1979

A molecular dynamics simulation of an aqueous ammonium chloride solution has been carried out at a mass density of 1.027 g/cm^3 , corresponding to a 2.2 m solution, and at a temperature of $T = 301 \text{ K}$. The effective pair potentials are based on the ST2 model of water, a rigid tetrahedral four point charge model of NH_4^+ and a single point charge model of Cl^- . The calculated structural properties of this solution are discussed and compared with those obtained for alkali halide solutions. The first hydration shell of the ammonium ion contains on the average eight water molecules, it has a more complex structure than the hydration shells of cations with spherical symmetry. The static orientational order of water dipole moments indicate a structure breaking ability of NH_4^+ .

I. Introduction

In the preceding papers of this series molecular dynamics simulations of alkali halide solutions have been reported and the discussion was restricted mainly to structural properties of these solutions. The simplifications employed in dealing with long range forces did not allow runs stable enough over times necessary to calculate dynamical properties with sufficient accuracy. The problems connected with these simulations are discussed in detail elsewhere [1].

The results achieved so far for selected alkali halide solutions with the ST2 water model justify improved and extended simulations at the expense of significantly more computer time. The far ranging interactions between the various particles are treated in the following way: The Ewald method is employed for ion-ion interactions [2]. The ion-water and water-water interactions are cut-off at a sphere with a radius of half the side-length of the basic cube. Then the forces are modified by the addition of a constant force in such a way that they become zero at the surface of this sphere, and the modified pair potentials (also set zero at the cut-off distance) are determined through integration of the new forces [3]. The point charges involved in the ion-water and water-water interactions are treated separately when inside the cut-off sphere. In the simulations before, all point charges of the ST2 model were included in the calculation of the forces

as long as the oxygen atom was inside the cut-off sphere and excluded when outside. Furthermore a four parameter version of quaternions [4] is employed in solving the Euler-Lagrange equations of the rotational motion.

The simulations are extended to include cations with a nonspherical charge distribution. The choice of NH_4^+ was led from a practical point of view: The similarity of NH_4^+ and H_2O allows easily to set up effective pair potentials for the ammonium ion. They have almost identical masses, bond angles and interatomic distances. Water molecule and ammonium ion are isoelectronic and also the electronic forces exerted on their neighbors are similar. The ammonium ion in a 2.2 molal NH_4Cl solution is modelled as a regular tetrahedron with point charges at the positions of the hydrogen atoms. In this paper the effective pair potentials and the improvements in the simulation are reported in detail and the structural properties of the NH_4Cl solution are discussed. In a subsequent paper the dynamical properties of this solution will be treated on the basis of various time correlation functions.

II. Effective Pair Potentials

Again the ST2 water model [5] is employed for the simulation of the NH_4Cl solution, while the chloride ion is described by a Lennard-Jones (LJ) sphere with a point charge in the center, and with LJ parameters as before [6]. The NH_4^+ is modelled as a regular tetrahedron with a N-H distance of 1.05 \AA , known from x-ray and neutron diffraction studies [7], resulting in a moment of inertia $I = 4.9 \cdot 10^{-40} \text{ g cm}^2$. A LJ sphere with the same

Reprint request to Dr. K. Heinzinger, Max-Planck-Institut für Chemie, Saarstr. 23, P.O.B. 3060, D-6500 Mainz.

0340-4811 / 79 / 0700-0840 \$ 01.00/0



Dieses Werk wurde im Jahr 2013 vom Verlag Zeitschrift für Naturforschung in Zusammenarbeit mit der Max-Planck-Gesellschaft zur Förderung der Wissenschaften e.V. digitalisiert und unter folgender Lizenz veröffentlicht: Creative Commons Namensnennung-Keine Bearbeitung 3.0 Deutschland Lizenz.

Zum 01.01.2015 ist eine Anpassung der Lizenzbedingungen (Entfall der Creative Commons Lizenzbedingung „Keine Bearbeitung“) beabsichtigt, um eine Nachnutzung auch im Rahmen zukünftiger wissenschaftlicher Nutzungsformen zu ermöglichen.

This work has been digitalized and published in 2013 by Verlag Zeitschrift für Naturforschung in cooperation with the Max Planck Society for the Advancement of Science under a Creative Commons Attribution-NoDerivs 3.0 Germany License.

On 01.01.2015 it is planned to change the License Conditions (the removal of the Creative Commons License condition "no derivative works"). This is to allow reuse in the area of future scientific usage.

parameters as in the ST2 water model is centered at the nitrogen atom position. The charge distribution is chosen to be 4 point charges of $+0.25$ elementary charges at each of the hydrogen atom positions. From experimental or theoretical points of view no support, neither for this nor for any other charge distribution useful for computer simulation of the ammonium ion, could be found in the literature.

With these models for the water molecules and the ions it is easy to formulate the effective pair potentials for the six different kinds of interactions: $\text{NH}_4^+-\text{NH}_4^+$, Cl^--Cl^- , $\text{NH}_4^+-\text{Cl}^-$, $\text{NH}_4^+-\text{water}$, Cl^--water , and water-water . All six pair potentials consist of a LJ term

$$V_{ij}^{\text{LJ}}(r) = 4\epsilon_{ij}[(\sigma_{ij}/r)^{12} - (\sigma_{ij}/r)^6] \quad (1)$$

and different Coulomb terms for Cl^--Cl^- interactions,

$$V_{--}^{\text{C}}(r) = e^2/r, \quad (2)$$

for $\text{Cl}^--\text{NH}_4^+$ and Cl^--water interactions,

$$V_{-i}^{\text{C}}(d_{-\alpha_i}) = -\sum_{\alpha_i=1}^4 q_{\alpha_i} e/d_{-\alpha_i}, \quad (3)$$

and for $\text{NH}_4^+-\text{NH}_4^+$, $\text{NH}_4^+-\text{water}$ and water-water interactions,

$$V_{ij}^{\text{C}}(d_{\alpha_i\alpha_j}) = S(r) \sum_{\alpha_i, \alpha_j=1}^4 q_{\alpha_i} q_{\alpha_j} / d_{\alpha_i\alpha_j}, \quad (4)$$

where i and j refer either to ions or water molecules, while r and $d_{\alpha_i\alpha_j}$ denote distances between LJ centers and point charges on different particles i and j , respectively. The switching function $S(r)$ in (4) has been introduced by Rahman and Stillinger [8] in order to reduce unrealistic Coulomb forces between very close water molecules. It is employed here for $\text{NH}_4^+-\text{water}$ interactions too, but not effective for $\text{NH}_4^+-\text{NH}_4^+$ interactions. The q_{α_i} denote point charges either on the water molecule ($\pm 0.23 e$) or on the ammonium ion ($+0.25 e$), where e is the elementary charge. The various Coulomb terms have the correct sign if it is agreed on that in the case of the water molecule $q_{\alpha_i} = +0.23 e$ for $\alpha_i = 1, 2$ and $q_{\alpha_i} = -0.23 e$ for $\alpha_i = 3, 4$. The LJ parameters for the various interactions are given in Table 1.

The simple cut-off procedure for ion-water and water-water interactions as applied in previous simulations has led to jumps in the potential energy and forces each time a particle crossed the cut-off sphere and resulted in trends in the average kinetic energy [1]. This problem can be overcome by the

Table 1. Lennard-Jones parameters of the various pair potentials for a NH_4Cl solution. σ is given in Å (first row) and ϵ in units of 10^{-16} erg.

| | $\text{H}_2\text{O}, \text{NH}_4^+$ | Cl^- |
|-------------------------------------|-------------------------------------|---------------|
| $\text{H}_2\text{O}, \text{NH}_4^+$ | 3.10 52.61 | 4.02 30.83 |
| Cl^- | — | 4.86 27.87 |

so called “shifted force potential” as proposed by Streett et al. [3]. The force between two particles is modified in such a way that it becomes zero at the cut-off distance. The new potential is determined from this modified force by integration, and the integration constant is chosen so that the potential is also zero at the surface of the cut-off sphere. If the pair potentials employed in the simulation of the NH_4Cl solution (1)–(4) consist only of terms which decrease with a power of $1/r$, which is our case, one has:

$$V(\mathbf{r}) = A/r^n, \quad \mathbf{F}(\mathbf{r}) = \frac{nA}{r^{n+1}} \cdot \frac{\mathbf{r}}{r}. \quad (5)$$

In order to achieve that the magnitude of the modified force $|\mathbf{F}_M(\mathbf{r})|$ becomes zero at the cut-off distance r_c , a central force $\mathbf{H}(\mathbf{r})$ has to be subtracted from $\mathbf{F}(\mathbf{r})$. The magnitude of $\mathbf{H}(\mathbf{r})$ is given by

$$H = \frac{nA}{r_c^{n+1}} \left(\frac{r}{r_c} \right)^m. \quad (6)$$

For the simulation reported here the simplest modification $m=0$ or $H = \text{const}$ was chosen. The new force is then given by

$$\begin{aligned} \mathbf{F}_M(\mathbf{r}) &= nA \left(\frac{1}{r^{n+1}} - \frac{1}{r_c^{n+1}} \right) \frac{\mathbf{r}}{r}, \quad |\mathbf{r}| \leq r_c, \\ \mathbf{F}_M(\mathbf{r}) &= 0, \quad |\mathbf{r}| > r_c, \end{aligned} \quad (7)$$

and the new pair potential by

$$\begin{aligned} V_M(\mathbf{r}) &= V(\mathbf{r}) + nA r/r_c^{n+1} + C, \quad |\mathbf{r}| \leq r_c, \\ V_M(\mathbf{r}) &= 0, \quad |\mathbf{r}| > r_c \end{aligned} \quad (8)$$

with

$$C = -V(r_c) - nA/r_c^n. \quad (9)$$

As for the ion-ion interaction the Ewald method [2] is employed, such shifted force potentials are only applied in the case of ion-water and water-water interactions. This modification of the pair potentials seems to be acceptable in view of all the other uncertainties in the choice of the models for the various particles.

III. Details of the Calculations

The basic periodic cube contained 200 water molecules, 8 ammonium and 8 chloride ions, equivalent to a 2.2 molal solution. With an experimental density of 1.027 g/cm^3 a sidelength of the basic cube of 18.66 \AA resulted.

The replacement of an alkali ion by the non-spherically symmetric ammonium ion did not require a change in the algorithm (including quaternion parameter) employed in the numerical integration of the dynamical equations of motion as discussed in detail in a previous paper [1]. The instability problems which prevented simulations stable enough over time ranges necessary for the calculation of dynamical properties with sufficient accuracy resulted solely from the cut-off procedures for ion-water and water-water interactions. An extension of the Ewald method — applied for ion-ion interactions — to all other interactions was excluded because of the large amount of computer time required for sufficiently accurate calculations. Instead of a less computer time consuming but less accurate calculation of the Ewald sum through interpolation of a table, the shifted force potential as described in the previous section was preferred. The radius of the cut-off sphere for ion-water as well as water-water interaction was chosen to be half of the sidelength of the basic cube.

In spite of the employment of the shifted force potential small energy jumps and a drift in total energy remained as long as the contribution of the point charges to energy and forces was solely decided by the distance of the corresponding LJ centers as in previous simulations. If this distance was smaller than the cut-off distance the contributions of all point charges were included,

otherwise excluded, independently of the real distance of the point charges. The desired stability was reached in this simulation by applying the minimum distance condition to each point charge and each LJ center separately: the real distance of two point charges and of two LJ centers is decisive for their contribution to force and energy.

The time step for the integration of the equations of motion could be enlarged by a factor of two compared with previous simulations to $\Delta t = 2.18 \cdot 10^{-16} \text{ sec}$. The results reported here and in the subsequent paper are from a simulation over 16340 time steps equivalent to a total elapsed time of 3.5 picoseconds. The fluctuation of the total energy $\Delta E/E$ over the whole run was smaller than $3 \cdot 10^{-5}$. The average value of the temperature was 301 K. There was no trend in the temperature and the deviation from the average value was smaller than $\pm 45 \text{ K}$ at any time step.

IV. Results and Discussion

a) Radial Distribution Functions

In Figs. 1–3 the radial distribution functions $g_{\text{NO}}(r)$, $g_{\text{NH}}(r)$, $g_{\text{ClO}}(r)$, $g_{\text{ClH}}(r)$, and $g_{\text{OO}}(r)$ — giving the oxygen and hydrogen atom densities about the NH_4^+ , Cl^- and the oxygen atoms relativ to the mean density of water — are shown together with the corresponding running integration numbers as defined by

$$n_{xy}(r) = 4\pi \rho_0 \int_0^r g_{xy}(r') r'^2 dr', \quad (10)$$

where ρ_0 is the number density of the water molecules. Some characteristic values of the various radial distribution functions (RDF) are given in Table 2.

Table 2. Characteristic values of the radial pair distribution functions $g_{xy}(r)$ for the ammonium chloride solution. R_i , r_{mi} and r_{m1} give the distances in \AA where for the i -th time $g_{xy}(r)$ is unity (two for $y = \text{H}$), has a maximum and a minimum, respectively. The values for pure water (in parenthesis) are taken from Stillinger and Rahman [5] resulting from a simulation for 41°C . The uncertainties in R_i , r_{M1} and r_{m1} are smaller than $\pm 0.02 \text{ \AA}$ except for r_{m1} of g_{00} which is uncertain as all the r_{M2} by about $\pm 0.1 \text{ \AA}$. The accuracy of the g values is estimated to be better than ± 0.05 , while the uncertainties of the $n(r_{m1})$ -values is about ± 0.2 , resulting from uncertain r_{m1} distances.

| xy | R_1 | r_{M1} | $g_{xy}(r_{M1})$ | R_2 | r_{m1} | $g_{xy}(r_{m1})$ | r_{M2} | $g_{xy}(r_{M2})$ | $n(r_{m1})$ |
|------|--------|----------|------------------|--------|----------|------------------|----------|------------------|-------------|
| NO | 2.82 | 3.05 | 6.85 | 3.35 | 3.68 | 0.31 | 5.06 | 1.44 | 8.1 |
| NH | 3.07 | 3.50 | 8.90 | 4.08 | 4.52 | 1.42 | 5.72 | 2.82 | 15.7 |
| ClO | 2.95 | 3.22 | 4.22 | 3.60 | 3.87 | 0.50 | 5.30 | 1.24 | 8.2 |
| ClH | 2.03 | 2.24 | 7.06 | 2.71 | 2.99 | 0.82 | 3.61 | 3.20 | 7.8 |
| OO | 2.63 | 2.85 | 2.86 | 3.23 | 3.62 | 0.84 | 4.86 | 1.06 | 5.2 |
| | (2.63) | (2.86) | (3.02) | (3.21) | (3.53) | (0.75) | (4.74) | (1.08) | |

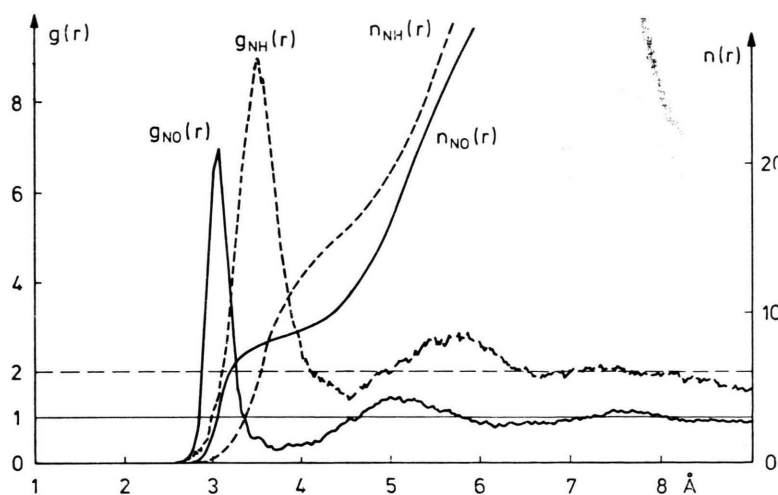


Fig. 1. Radial distribution functions and running integration numbers for ammonium-oxygen (full line) and ammonium-hydrogen (dashed) in a 2.2 molal NH_4Cl solution. In computing $g_{\text{NH}}(r)$ only the hydrogens belonging to water molecules were included.

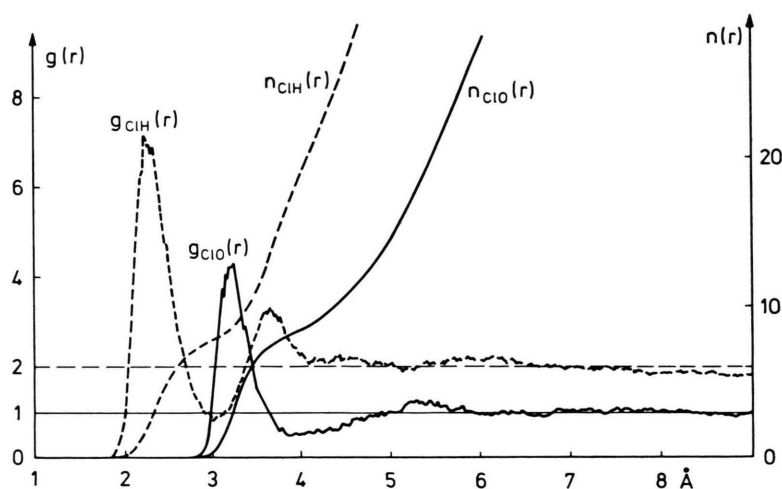


Fig. 2. Radial distribution functions and running integration numbers for chloride-oxygen (full line) and chloride-hydrogen (dashed) in a 2.2 molal NH_4Cl solution.

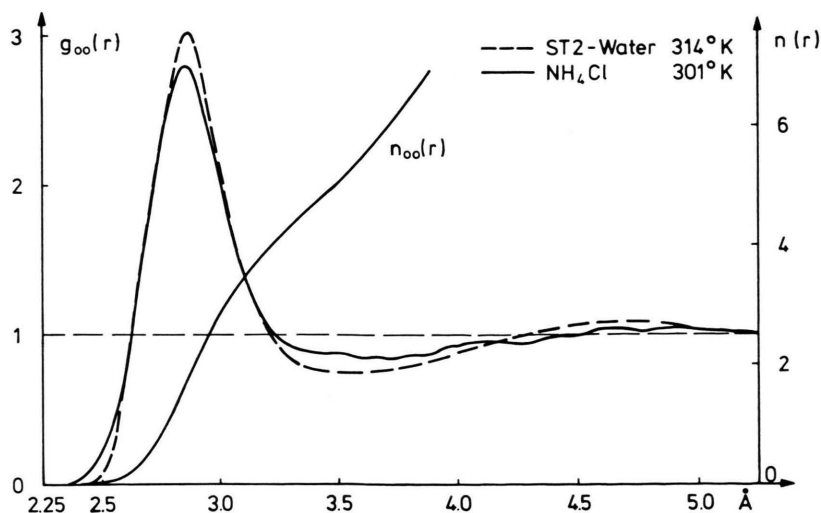
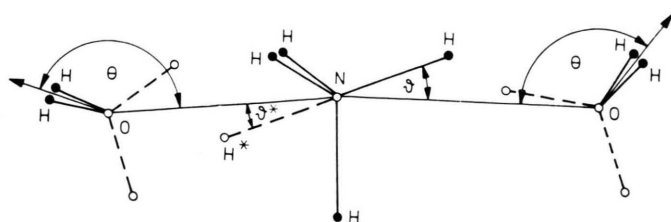


Fig. 3. Oxygen-oxygen radial distribution function and running integration number in a 2.2 molal NH_4Cl solution at 28 °C (full line) and in pure water [5] (dashed) for 31 °C.

Fig. 4. Definition of the angles ϑ , ϑ^* and θ .

Comparing $g_{\text{NO}}(r)$ with alkali ion-oxygen RDF as reported in a previous paper [9], the NH_4^+ is positioned between Na^+ and Cs^+ (simulations with K^+ and Rb^+ are not available for comparison). The characteristic ion-oxygen distances of the first peak in $g_{\text{NO}}(r)$ are slightly smaller (about 0.1 Å), its height is enlarged by about a factor of 1.5 and the first minimum more pronounced when compared with Cs^+ . The indication of a second hydration shell is similar to that for Na^+ . The existence of features of $g_{\text{CSO}}(r)$ and $g_{\text{NaO}}(r)$ in $g_{\text{NO}}(r)$ results from the size of NH_4^+ and the charge distribution — 0.25 elementary charges at the hydrogen atom positions — which leads to a well defined first hydration shell and well oriented water molecules, allowing the formation of a second hydration shell. The orientation of the water molecules in the hydration shells is discussed in detail below.

Preliminary simulations without the shifted force potential indicate the influence of the shift on the RDF. With the normal cut-off procedure the maxima of the first peaks in $g_{\text{NO}}(r)$ and $g_{\text{OO}}(r)$ coincided at (2.95 ± 0.05) Å — the ammonium ion and the water molecule have the same LJ parameters — while they moved apart after the introduction of the shifted force potential to 2.85 Å and 3.05 Å for $g_{\text{OO}}(r)$ and $g_{\text{NO}}(r)$, respectively, as can be seen from Table 1. This shift effects mainly the interactions of two particles with point charges not placed at the LJ centers. A change of $g_{\text{ClO}}(r)$ could not be recognized.

The hydration number for the ammonium ion — $n_{\text{NO}}(r_{\text{m1}})$ — of 8.1 together with the rather narrow first peak in $g_{\text{NO}}(r)$ implies an angular distribution of the water molecules in the hydration shell of NH_4^+ where four water molecules are located near the N-H directions and the remaining four near the invers directions N-H* (see Fig. 4), but all in similar distances from the ion. The two groups of water molecules, however, should differ significantly in some of their properties, because one group is positioned opposite to point charges

and the other one not. The separation into the two groups has been achieved in the following way: For all eight water molecules the angle ϑ (for definition see Fig. 4) has been calculated and to each of the hydrogen atoms of the NH_4^+ the water molecule with the smallest angle ϑ has been attributed. The remaining four water molecules form the second group. On the basis of this separation the two groups have been treated separately. In Fig. 5 the distribution of $\cos \vartheta$ for the water molecules of the first group together with the $\cos \vartheta^*$ distribution for the water molecules of the second group (dashed) are shown. It is obvious from this Figure that the point charges at the ammonium ion enforce a narrow distribution centered around $\vartheta = 0$. The water molecules in the N-H* directions show a broad distribution of the angle ϑ^* between zero and half of a tetrahedral angle, with a preference for small ϑ^* . The difference in the orientation for the two groups of water molecules — given by θ — is discussed in detail below.

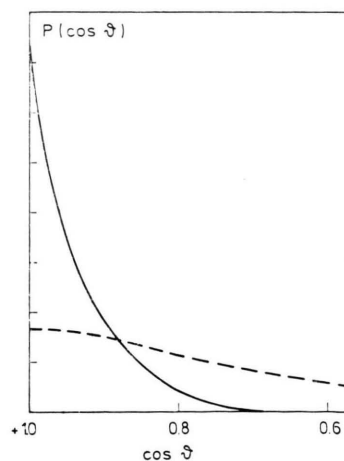


Fig. 5. Angular distribution of the water molecules in the hydration shell of the ammonium ion. The distribution of the first and second group of water molecules is given as a function of $\cos \vartheta$ (full line) and of $\cos \vartheta^*$ (dashed), respectively. For further explanation see text.

$g_{\text{ClO}}(r)$ and $g_{\text{ClH}}(r)$ differ significantly from the previously reported ones [9, 10], where the choice of the same LJ parameters for isoelectronic cations and anions had led to a discrepancy between diffraction results and the computer simulation. The evaluation of improved LJ parameters for the halide ions is described in a previous paper [6]. It has been shown that the new parameters lead to agreement between the simulation of a 2.2 molal NaCl solution and corresponding x-ray diffraction measurements if the position of the first maximum in $g_{\text{ClO}}(r)$ is compared with the average ion-oxygen distance as determined from a First Neighbor Model fit to the x-ray structure function. There is no significant difference between the NaCl and the NH_4Cl solutions as far as the hydration complex of the chloride ions is concerned. Therefore the newly determined characteristic values for $g_{\text{ClO}}(r)$ and $g_{\text{ClH}}(r)$ as given in Table 1 can be considered reliable.

It is interesting to note that recent Monte Carlo studies of aqueous solutions of alkali chlorides by Beveridge and coworkers [11] result in a chloride-oxygen RDF which agrees in the characteristic distances (R_1 , R_2 , r_{M1} , r_{M2} and r_{m1}) with the one shown in Fig. 2, although these authors employed pair potentials for water-water as well as for ion-water interactions which were derived from the ab initio calculations of Clementi and coworkers [12]. The height of the first maximum in $g_{\text{ClO}}(r)$ from the Monte Carlo studies is lower by a factor of about 0.7 while $g_{\text{ClO}}(r_{\text{M2}})$ is slightly higher when compared with this simulation, and consequently a small difference in the hydration numbers — when defined as $n_{\text{ClO}}(r_{\text{m1}})$ — exists: 8.2 ± 0.2 from the MD and 7.7 ± 0.3 from the MC calculations. The question if the difference in the height of the maxima has to be attributed totally to differences in the pair potentials can not be answered unambiguously because the concentration for which the MC calculations have been performed has not been given in the paper. In addition the different counterions could partly be responsible for the differences.

The RDF for oxygen-oxygen is in its characteristic values, as shown in Table 1, positioned between $g_{\text{OO}}(r)$ for the alkali halide solutions and the one for pure ST2 water. It is compared in Fig. 3 with $g_{\text{OO}}(r)$ for pure ST2 water at 41 °C as reported by Stillinger and Rahman [5]. Again it is obvious that the addition of electrolytes changes

the water structure in the same way as increasing temperature does, an often recognized effect.

The structure of aqueous ammonium halide solutions has been investigated by x-ray diffraction [13]. The RDF for the total system has been reported only, and a direct comparison of $g_{\text{NO}}(r)$ and $g_{\text{OO}}(r)$ can not be performed. The diffraction measurements lead to a first maximum in $g(r)$ at 2.91 Å, while from the simulation maxima at 2.87 Å for $g(r)$, at 2.85 Å for $g_{\text{OO}}(r)$, and 3.05 Å for $g_{\text{NO}}(r)$ result. The experimentally determined average chloride-water distance of 3.2 Å is in agreement with the position of the first maximum from the simulation at 3.22 Å.

b) Orientation of the Water Molecules

The orientation of the water molecules in the neighborhood of the ions can be seen from the relative positions of the first peaks in the ion-oxygen and ion-hydrogen radial distribution functions as shown in Fig. 1–2, from the distribution of $\cos \theta$ for the water molecules in the first hydration shell of the ions, and from the average value of $\cos \theta$ as a function of distance as given in Figures 6–8. θ is defined as the angle between the dipolemoment direction of the water molecule and the vector pointing from the oxygen atom towards the center of the ion (Figure 4).

The distance between the first peaks of $g_{\text{ClH}}(r)$ and $g_{\text{ClO}}(r)$ is 1 Å, the O–H distance in the rigid ST2 model, and in addition $n_{\text{ClO}}(r_{\text{m1}})$ and $n_{\text{ClH}}(r_{\text{m1}})$ have almost the same value. This allows the conclusion drawn already from previous simulations that preferentially a linear hydrogen bond is formed with the chloride ion. This orientation of the water molecules in the neighborhood of the chloride ion has also been found from x-ray and neutron diffraction studies [14, 15]. NMR investigations have led to the same conclusion for the fluoride ion [16]. In the case of cations the distance between the first peaks of $g_{\text{NO}}(r)$ and $g_{\text{NH}}(r)$ of 0.45 Å together with $n_{\text{NH}}(r_{\text{m1}}) \approx 2n_{\text{NO}}(r_{\text{m1}})$ indicates similarly that preferentially a lone pair orbital is directed towards the ammonium ion. But the picture of the hydration shell of NH_4^+ is more complex than for the spherically symmetric alkali ions as mentioned above, and as can be seen from Figures 6–8.

The distribution of $\cos \theta$ for the water molecules in the first hydration shells of the ammonium and

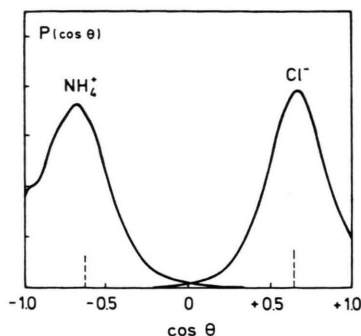


Fig. 6. Angular distribution of the water dipoles in the hydration shells of the ammonium and the chloride ion. The dashed marks indicate the mean value of $\cos \theta$. The distributions are normalized and given in arbitrary units.

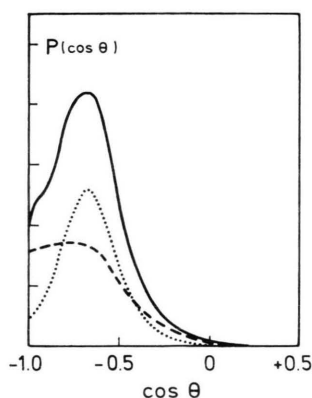


Fig. 7. Separation of the angular distribution of the water dipoles in the hydration shell of the ammonium ion into the distributions from the four water molecules opposite of point charges (points) and the remaining four (dashed).

the chloride ion is shown in Figure 6. The distributions are centered around $+0.6$ for Cl^- and -0.6 for NH_4^+ , in agreement with the conclusion drawn above that preferentially a linear hydrogen bond is formed with the chloride ion and a lone pair orbital is directed towards the ammonium ion. Although NH_4^+ is smaller than Cl^- , its $P(\cos \theta)$ is significantly broader. The explanation for this different behavior can be seen from Fig. 7, where the distribution is subdivided into the contributions of the two groups of water molecules in the hydration shell of the ammonium ion as described above. The four water molecules opposite to the point charges have a rather narrow distribution (points) as expected, while $P(\cos \theta)$ for the other four water molecules (dashed) has an almost constant value in the range $-1 < \cos \theta < -0.6$ and then decreases slowly even reaching positive values of $\cos \theta$. This distribution for the second group of water molecules results from the fact that their orientation is not determined mainly by the point charges of the ammonium ion but rather by the charges of the surrounding water molecules.

The average values of $\cos \theta$ as a function of distance from the ammonium and the chloride ion are shown in Figure 8. For the chloride ion (upper part) $\langle \cos \theta(r) \rangle$ has at small distances a value of about $+0.6$, corresponding to half of a tetrahedral angle, the orientation of the waters in the first hydration shell as concluded above. With increasing distance $\langle \cos \theta(r) \rangle$ decreases more slowly than it has been found from previous simulations of alkali

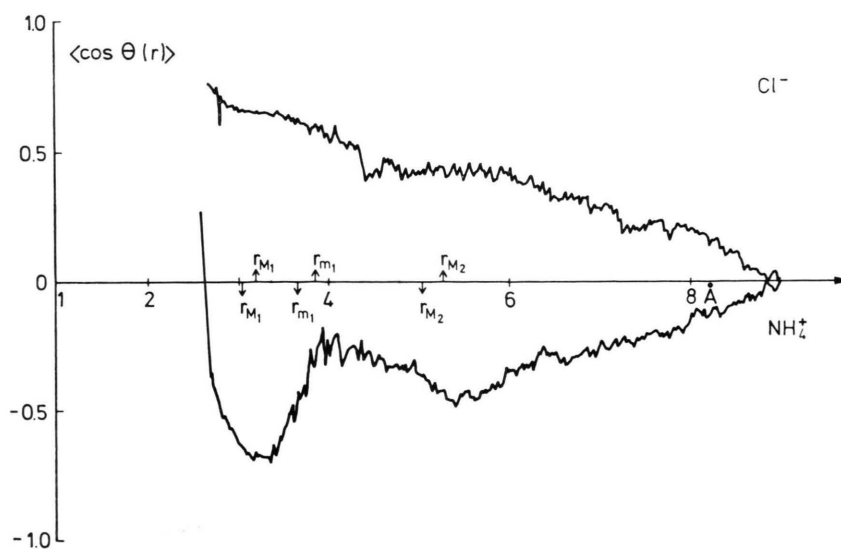


Fig. 8. Average value of $\cos \theta$ as a function of distance from the chloride (upper part) and the ammonium ion. The definition of θ is given in Figure 4.

chloride solutions [9]. This long range ordering of the water molecules around the chloride ion could be a consequence of the structure breaking ability of the NH_4^+ . The characteristic feature of the average value of $\cos \theta$ as a function of distance from the ammonium ion (lower part of Fig. 8) is the decrease of $\langle \cos \theta(r) \rangle$ at distances smaller than r_{M1} . In the case of the spherically symmetric alkali ions $\langle \cos \theta(r) \rangle$ was rather constant at distances smaller than R_2 with a value of about -0.6 , and the less oriented water molecules were located at larger distances. The occurrence of water molecules with energetically unfavorable orientations at small distances from NH_4^+ is a consequence of the existence of the second group of water molecules in the hydration shell of the NH_4^+ , water molecules which are not located opposite of point charges.

The average value of the cosine of the angle between the dipole moments of two water molecules in the NH_4Cl solution is given as a function of distance between the oxygen atoms of the two water molecules in Figure 9. It resembles strongly the result for the LiJ solution and is significantly different from the one for other alkali chloride and alkali fluoride solutions, where $\langle \cos \theta_{ww}(r) \rangle$ starts also between 0.5 and 0.6, equivalent to about half of tetrahedral angle, but falls off much faster, reaching zero between 3 and 4 Å and remains negative for larger distances [9]. This different behavior becomes obvious if it is discussed in connection with the quantity $\langle \mathbf{M}^2 \rangle / N$, where \mathbf{M} is defined by

$$\mathbf{M} = \sum_i^N \mathbf{m}_i \quad (11)$$

and \mathbf{m}_i is the unit vector in the dipole moment direction of water molecule i . The sum extends over all the $N=200$ water molecules in the basic cube.

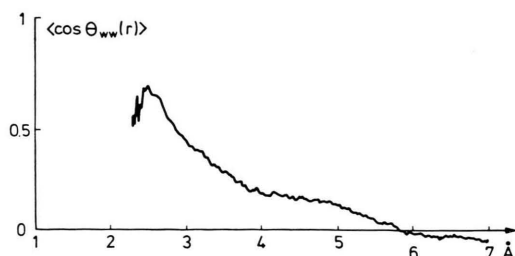


Fig. 9. Average value of $\cos \theta_{ww}(r)$ as a function of distance between the oxygen atoms of two water molecules in the NH_4Cl solution. θ_{ww} is the angle between the dipole moment vectors of the two water molecules.

Table 3. Comparison of $\langle \mathbf{M}^2 \rangle / N$ for the NH_4Cl solution with the ones for various 2.2 molal alkali halide solutions from previous simulations [9] and pure ST2 water [5]. The value in parenthesis is uncertain as it results from a simulation run over 500 time steps only.

| Solute | NH_4Cl | LiJ | LiCl | NaCl |
|------------------------------------|------------------------|--------------|----------------|---------------|
| $\langle \mathbf{M}^2 \rangle / N$ | 0.79 | 0.44 | 0.34 | 0.32 |
| Solute | CsCl | CsF | pure ST2 water | |
| $\langle \mathbf{M}^2 \rangle / N$ | (0.39) | 0.17 | 0.15 | |

In Table 3 the value of $\langle \mathbf{M}^2 \rangle / N$ for the NH_4Cl solution is compared with simulation results for various alkali halide solutions and pure ST2 water. It is obvious that $\langle \mathbf{M}^2 \rangle / N$ depends only on the anions as far as the alkali halide solutions are concerned and increases with increasing ion size, where the value for the fluoride ion is very similar to the one for pure water. As increasing anion size means increasing structure breaking ability; the large value of 0.79 indicates that the combined structure beaking effect of the NH_4^+ and Cl^- far exceeds the one for the large iodide ion. $\langle \mathbf{M}^2 \rangle / N = 1$ would mean completely uncorrelated water dipole directions.

c) Average Potential Energy and Pair Interaction Energy Distribution

The average potential energy of a water molecule in the field of an ammonium and a chloride ion is shown in Fig. 10 as a function of ion-oxygen distance. The dashed line, giving $\langle V_{\text{ClW}}(r) \rangle$, is significantly different from previously reported ones [9], because of the improved LJ parameters for the chloride ion. The new parameters, which have led to a shift of the first maximum in $g_{\text{ClO}}(r)$ to a larger distance as discussed above, result in a similar shift of the minimum of $\langle V_{\text{ClW}}(r) \rangle$, and consequently the depth of the minimum is lowered by almost a factor of two. This difference in the average potential energy is, of course, reflected in the chloride ion-water pair interaction energy distributions, shown as dashed line in Figure 11. The maximum at the negative energy side of the distribution is shifted to less negative values and is less pronounced when compared with previous simulations. Position and depth of the minimum in $\langle V_{\text{NH}_4\text{W}}(r) \rangle$ are similar to the ones for Cs^+ . The existence of positive energy values at small distances is a new feature, which

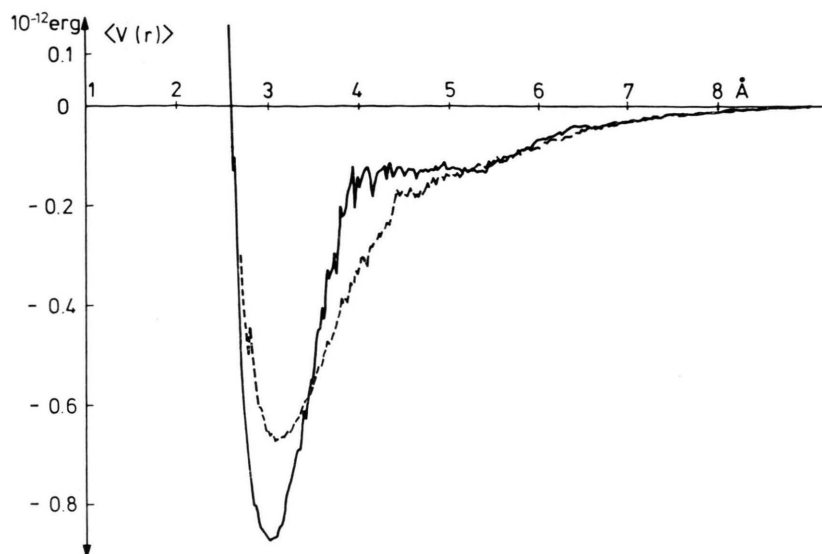


Fig. 10. Average potential energy of a water molecule in the field of the ammonium ion (full line) and the chloride ion (dashed) as a function of ion-oxygen distance.

results from the water molecules in positions not opposite of point charges. There can be water molecules with energetically unfavorable orientations relative to the point charges of the NH_4^+ . It is interesting to note that the average potential energy of the water molecules is for distances larger than 5 Å practically the same for the chloride and the ammonium ion although in one case the charge is located at the center of the ion while in the other case one quarter of an elementary charge is positioned at each of the four hydrogen atom positions. The pair interaction energy distribution for NH_4^+ -water (full line in Fig. 11) shows that the hydration shell of NH_4^+ is more pronounced than the one for

Cs^+ but significantly less than in the case of the Na^+ . There exists a larger number of water molecules with positive energies when compared with Cl^- , again a consequence of the two groups of water molecules in the hydration shell of NH_4^+ , as discussed above.

The average potential energy of two water molecules is shown in Fig. 12 as a function of oxygen-oxygen distances and the corresponding pair interaction energy distribution is given in Figure 13. $\langle V_{\text{ww}}(r) \rangle$ is not significantly different from the ones for the other alkali halide solutions as reported in a previous paper [9]. The positive energy part between 3.5 and 4.5 Å is very similar to

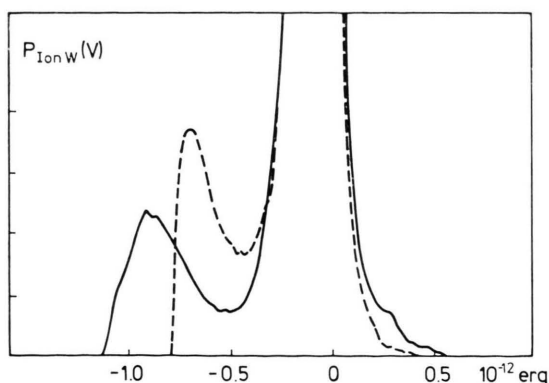


Fig. 11. Pair interaction energy distribution for ammonium ion-water (full line) and chloride ion-water (dashed). $P(V)$ is given in arbitrary units.

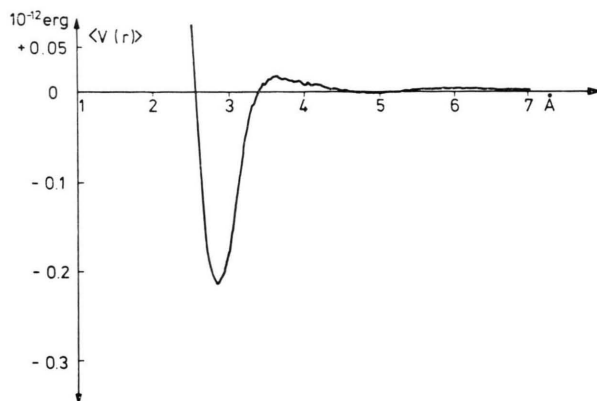


Fig. 12. Average potential energy of the water molecules as a function of oxygen-oxygen distance in a NH_4Cl solution.

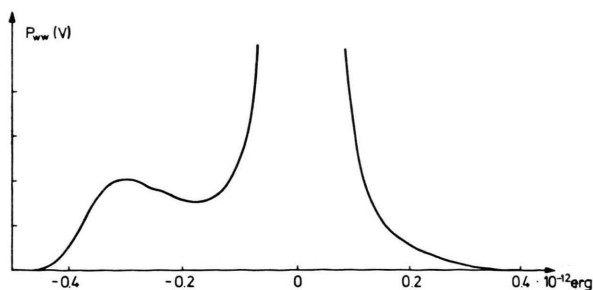


Fig. 13. Pair interaction energy distribution for water-water in an ammonium chloride solution. $P(V)$ is given in arbitrary units.

the case of the LiJ solution, a similarity between the two solutions which has been recognized above already and which results from the stronger structure breaking ability of J^- relative to the other halide ions. The positive part of the water-water energy distribution is similar to that of the CsCl solution. The less orienting power of the ammonium ion compared with the small alkali ions forces a smaller number of water molecules to energetically unfavorable orientations relative to each other. This effect also leads to a slightly more pronounced peak at the negative energy side of the distribution.

d) Closing Remarks

It should be stressed that the above discussion of the structure of the NH_4Cl solution is based on the rigid four point charge model chosen for the ammonium ion. The available experimental information is very scarce and not sufficient to support or dismiss this model. Thus it remains open, if e.g. the subdivision of the water molecules in the hydration shell of NH_4^+ into two groups, based on a hydration number of eight, can be supported by experimental investigations. Improved x-ray and neutron diffraction studies might lead to significantly better information from this side on the radial distribution functions and on the orientation of the water molecules in the hydration sphere of NH_4^+ . A detailed comparison of the x-ray structure function with the one calculated from the simulation is in preparation.

These remarks on the structural properties of the NH_4Cl solution are similarly valid for the dynamical properties which will be discussed in a subsequent paper.

Helpful discussions with Dr. L. Schäfer and financial support by Deutsche Forschungsgemeinschaft are gratefully acknowledged.

- [1] K. Heinzinger, W. O. Riede, L. Schäfer, and Gy. I. Szász, ACS Symposium Series **86**, 1 (1978).
- [2] P. P. Ewald, Ann. Physik **64**, 253 (1921); see also: J. P. Valleau and S. G. Whittington, in: Modern Theoretical Chemistry, Vol. 5: Statistical Mechanics, Part A (B. J. Berne, ed.), Plenum Press, New York and London 1977.
- [3] W. B. Streett, D. J. Tildesly, and G. Saville, ACS Symposium Series **86**, 144 (1978).
- [4] D. J. Evans, Mol. Phys. **34**, 317 (1977).
- [5] F. H. Stillinger and A. Rahman, J. Chem. Phys. **60**, 1545 (1974).
- [6] G. Pálinkás, W. O. Riede, and K. Heinzinger, Z. Naturforsch. **32a**, 1137 (1977).
- [7] K. Kurki-Suonio, M. Merisalo, A. Vahvaselkä, and F. K. Larsen, Act. Cryst. A **32**, 110 (1976).
- [8] A. Rahman and F. H. Stillinger, J. Chem. Phys. **55**, 336 (1971).
- [9] K. Heinzinger and P. C. Vogel, Z. Naturforsch. **31a**, 463 (1976).
- [10] P. C. Vogel and K. Heinzinger, Z. Naturforsch. **31a**, 376 (1976).
- [11] D. L. Beveridge, M. Mezei, S. Swaminathan, and S. W. Harrison, ACS Symposium Series **86**, 191 (1978).
- [12] H. Kistenmacher, H. Popkie, and E. Clementi, J. Chem. Phys. **61**, 799 (1974).
- [13] A. H. Narten, J. Chem. Phys. **74**, 765 (1970).
- [14] A. H. Narten, F. Vaslow, and H. A. Levy, J. Chem. Phys. **58**, 5017 (1973).
- [15] A. K. Soper, G. W. Neilson, J. E. Enderby, and R. A. Howe, J. Phys. C.: Solid St. Phys. **10**, 1793 (1977).
- [16] H. G. Hertz and C. Rädle, Ber. Bunsenges. **77**, 521 (1973).